Sustainable Energy & Fuels

ROYAL SOCIETY OF CHEMISTRY

COMMUNICATION

View Article Online
View Journal | View Issue

Cite this: *Sustainable Energy Fuels*, 2025, **9**, 3791

Received 13th May 2025
Accepted 29th May 2025

DOI: 10.1039/d5se00676g

rsc.li/sustainable-energy

Unassisted visible-light–driven NADH regeneration based on a dual-photoelectrode system†

Koya Kano,[a] Masanobu Higashi *[b] and Yutaka Amao *[ac]

NADH regeneration is crucial for biocatalytic processes. One promising example is visible-light–driven NADH regeneration using water as an electron source. Here, we demonstrate for the first time, to the best of our knowledge, visible-light–driven electrochemical NADH regeneration using water as an electron source without the need for an external bias. This is achieved by combining an IrO_x/TaON (or RhO_x/TaON) photoanode, CdS/$CuInS_2$ photocathode and $[Cp^*Rh(bpy)(H_2O)]^{2+}$, as a catalyst for regioselective reduction of NAD^+. Furthermore, application of this system to the production of L-lactate from pyruvate using lactate dehydrogenase was attempted.

Reduced nicotinamide adenine dinucleotide (NADH) is widely used as a cofactor functioning as an electron donor in various reactions catalysed by oxidoreductases (*i.e.*, redox enzymes). Efficiently regenerating consumed cofactors (*e.g.*, reducing NAD^+ to NADH) is crucial for achieving a broad application of oxidoreductases because of their high cost, low stability, and the stoichiometric amount that needs to be supplied. Various ways of regenerating NADH, for example using biocatalytic, chemical,[1–3] electrochemical,[4–7] photochemical,[8–16] homogeneous catalytic,[17] and heterogeneous catalytic[18] methods, have been investigated. Among these methods, photochemistry has attracted particularly considerable attention in recent years because clean and abundant solar energy can be converted into chemical energy. It is therefore desirable to develop a visible-light–driven NADH-regeneration system. However, in the process of regenerating NADH, isomers (1,2- or 1,6-NADH) and dimeric NAD^+ are produced in addition to 1,4-NADH. Unlike 1,4-NADH, these isomers and dimeric NAD^+ have no function as a coenzyme for oxidoreductase, suppression of their production is an important issue for developing an NADH-regeneration system. Rh complex $[Cp^*Rh(bpy)(H_2O)]^{2+}$ (Cp^* = pentamethylcyclopentadienyl, bpy = 2,2′-bipyridyl) acting as a proton- and electron-transfer catalyst has been widely used and studied for the regiospecific reduction of NAD^+ to only 1,4-NADH.[19–22] Many NADH-regeneration systems using photocatalytic dye with $[Cp^*Rh(bpy)(H_2O)]^{2+}$ have been reported.[11–16] However, most light-driven NADH-regeneration systems require a sacrificial electron donor, such as triethanolamine (TEOA); so, it is desirable to develop an NADH-regeneration system that uses water as an electron source. Moreover, there are few stable semiconductor photocatalysts capable of catalyzing both water oxidation and $[Cp^*Rh(bpy)(H_2O)]^{2+}$ reduction under visible-light irradiation. With the aim of achieving visible-light-driven NADH regeneration using water as an electron source, a Z-scheme photoelectrochemical system using two semiconductor-based photoelectrodes (a photoanode and a photocathode) and $[Cp^*Rh(bpy)(H_2O)]^{2+}$, as shown in Fig. 1 was devised.

In this system, the reaction is broken up into two stages: one for reduction of $[Cp^*Rh(bpy)H_2O]^{2+}$ and the other for water oxidation. For $[Cp^*Rh(bpy)H_2O]^{2+}$ reduction system, the photoexcited electrons reduce $[Cp^*Rh(bpy)H_2O]^{2+}$, and the photogenerated holes received the photoexcited electrons from the water oxidation system. Conversely, for water oxidation

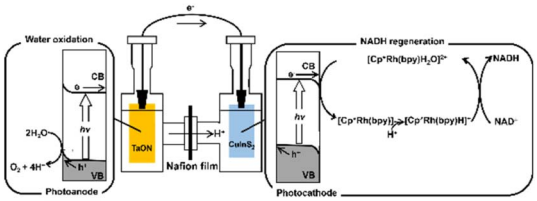

Fig. 1 Z-scheme mechanism of NADH regeneration using a system including a photoanode, a photocathode and $[Cp^*Rh(bpy)(H_2O)]^{2+}$ under visible-light irradiation.

[a]*Graduate School of Science, Osaka Metropolitan University, 3-3-138 Sugimoto, Sumiyoshi-ku, Osaka 558-8585, Japan*

[b]*Institutional Advancement and Communications, Kyoto University, Yoshida-Honcho, Sakyo-ku, Kyoto 606-8501, Japan*

[c]*Research Centre for Artificial Photosynthesis (ReCAP), Osaka Metropolitan University, 3-3-138 Sugimoto, Sumiyoshi-ku, Osaka 558-8585, Japan. E-mail: amao@omu.ac.jp*

† Electronic supplementary information (ESI) available: Experimental section, Additional data. See DOI: https://doi.org/10.1039/d5se00676g

system, the photogenerated holes oxidize water to O_2, and photoexcited electrons are injected into the valence band of the $[Cp^*Rh(bpy)H_2O]^{2+}$ reduction system. Note that the $[Cp^*Rh(bpy)H_2O]^{2+}$ reduction and water oxidation systems do not require water oxidation and $[Cp^*Rh(bpy)H_2O]^{2+}$ reduction, respectively. Therefore, various semiconductor materials can be used in the Z-scheme system.

In this study, $CuInS_2$ and TaON were employed as a photocathode and a photoanode, respectively. $CuInS_2$ has a small bandgap (1.5 eV), allowing visible-light absorption, and a relatively high (negative) conduction band level and therefore is used for various photocatalytic and photoelectrochemical reactions.[23–25] We recently reported that a CdS-modified $CuInS_2$ photocathode can reduce CO_2 to formate when combined with a biocatalyst system using formate dehydrogenase as the enzyme and methyl viologen as an artificial coenzyme, instead of NADH.[26] However, oxidation of water using $CuInS_2$ is not thermodynamically favored. Conversely, TaON, in addition to having a small bandgap (2.4 eV) allowing visible-light absorption, also has a valence band level for water oxidation. We reported photoelectrochemical water oxidation over a TaON photoanode under visible-light irradiation by loading an appropriate water oxidation cocatalyst, such as CoO_x, RhO_x and IrO_x.[27–29] In the current work, visible-light–driven electrochemical NADH regeneration using water as an electron source, without an external bias, was achieved by combining a TaON photoanode, a $CuInS_2$ photocathode, and $[Cp^*Rh(bpy)(H_2O)]^{2+}$. Its application to a subsequent biocatalytic reaction involving the production of L-lactate from pyruvate using the regenerated NADH and lactate dehydrogenase (LDH) were demonstrated here for the first time, to the best of our knowledge. The $CuInS_2$ and TaON electrodes were fabricated according to previously reported methods.[29,30] The $CuInS_2$ samples were modified with CdS using the chemical bath deposition method.[31] The resulting electrode was calcined at 673 K for 30 min under N_2 gas flow, with the obtained electrode denoted as CdS/$CuInS_2$. Water oxidation cocatalysts (5 wt% CoO_x, 0.7 wt% RhO_x and 1 wt% IrO_x, calculated as metal; optimal loadings for CoO_x[28] and RhO_x[29]) were each loaded onto TaON using the impregnation method, with the obtained samples denoted as CoO_x/TaON, RhO_x/TaON, and IrO_x/TaON, respectively. The electrochemical cell used for the photocurrent measurements consisted of a prepared electrode, Pt counter electrode, Ag/AgCl reference electrode, and phosphate buffer solution (pH = 7.0). In some cases, $[Cp^*Rh(bpy)(H_2O)]^{2+}$ (1.0 mM) was added to the solution. The potential of the working electrode was controlled using a potentiostat. The solution was purged with Ar gas for more than 20 min prior to the measurement. The electrodes were irradiated using a 300 W Xe lamp fitted with an L-42 cut-off filter. The detailed procedures are described in ESI.† Reduction properties of $[Cp^*Rh(bpy)(H_2O)]^{2+}$ over a CdS/$CuInS_2$ photocathode were investigated, as shown in Fig. 2. Without $[Cp^*Rh(bpy)(H_2O)]^{2+}$, the CdS/$CuInS_2$ photocathode exhibited a negative cathodic photoresponse at a potential more negative than approximately −0.1 V *vs.* Ag/AgCl. This photocurrent was probably derived from the reduction of H^+. In the case of the phosphate buffer solution to which $[Cp^*Rh(bpy)(H_2O)]^{2+}$ was

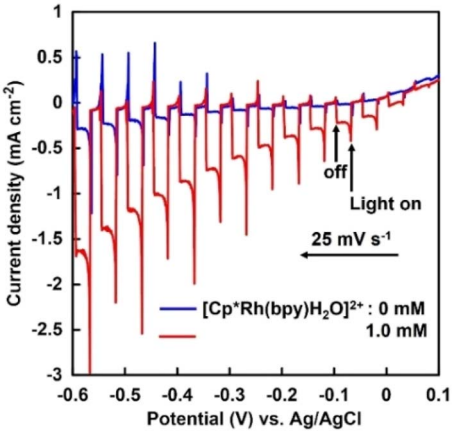

Fig. 2 Current–potential curves for the CdS/$CuInS_2$ photocathode in phosphate buffer solution (pH = 7.0) with and without $[Cp^*Rh(bpy)(H_2O)]^{2+}$ under chopped visible-light irradiation.

added, the photocurrent over the CdS/$CuInS_2$ photocathode significantly increased, strongly suggesting that the CdS/$CuInS_2$ photocathode reduced $[Cp^*Rh(bpy)(H_2O)]^{2+}$.

Next, reduction of NAD^+ to NADH was performed *via* $[Cp^*Rh(bpy)(H_2O)]^{2+}$ at −0.2 V *vs.* Ag/AgCl using a two-compartment cell divided by a Nafion membrane. $[Cp^*Rh(bpy)(H_2O)]^{2+}$ (1.0 mM) and NAD^+ (2.0 mM) were added to the solution of the cathode side. Generally, although it has been reported that 1,2-, 1,4-, 1,6-NADH isomers and NAD_2 are produced in the NAD^+ reduction, high-performance liquid chromatography analysis revealed that NAD^+ was selectively reduced to 1,4-NADH in our developed system, as shown in Fig. S1.† Hereafter, 1,4-NADH is simply denoted as NADH. Fig. 3 shows the time courses of photocurrent density and the amount of NADH produced over the CdS/$CuInS_2$ photocathode under visible-light irradiation.

Photocurrent density decreased from −0.41 to −0.18 mA cm^{-2} upon 30 min of irradiation and then remained almost constant for the next 150 min, as shown in the inset of Fig. 3. The amount of NADH produced increased linearly with time.

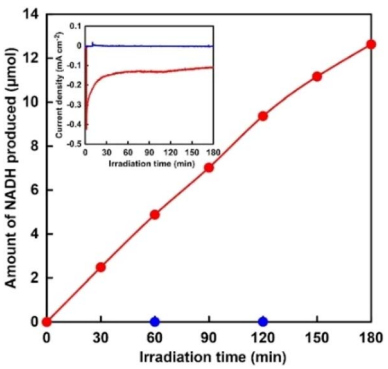

Fig. 3 Time dependence of NADH production with the CdS/$CuInS_2$ photocathode at −0.2 V *vs.* Ag/AgCl under visible-light irradiation. Inset: time dependence of photocurrent density. Red: in the presence of $[Cp^*Rh(bpy)(H_2O)]^{2+}$; blue: in the absence of $[Cp^*Rh(bpy)(H_2O)]^{2+}$.

The yield of NADH from NAD^+ was estimated to be 32% at 180 min of irradiation. No NADH production was observed in the absence of $[Cp^*Rh(bpy)(H_2O)]^{2+}$, indicating that the CdS/$CuInS_2$ photocathode cannot directly reduce NAD^+ to NADH. These results indicated that reduction of NAD^+ to NADH proceeded *via* $[Cp^*Rh(bpy)(H_2O)]^{2+}$ accepting the photoexcited electrons from the CdS/$CuInS_2$ photocathode. Photoelectrochemical water oxidation performance over the TaON photoanode was found to strongly depend on the kind of water oxidation cocatalyst used. Specifically, the influence of the three cocatalysts (*i.e.*, CoO_x, RhO_x, and IrO_x) on the photoelectrochemistry of the TaON photoanode was investigated. As shown in Fig. S2,† although all electrodes showed clear photoresponses in a wide range of potentials, different onset potentials of the photocurrent were observed. Specifically, the onset potentials of the CoO_x/TaON, RhO_x/TaON and IrO_x/TaON photoanodes were estimated to be approximately −0.45, −0.55, and −0.60 V *vs.* Ag/AgCl, respectively, with these values considerably more negative than that of the CdS/$CuInS_2$ photocathode (0.03 V *vs.* Ag/AgCl, as shown in Fig. 2). This result implied that the combination of cocatalyst-loaded TaON photoanode and CdS/$CuInS_2$ photocathode can enable photoelectrochemical NADH regeneration using water as an electron source without an external bias. Here, NADH regeneration using a photoelectrochemical cell consisting of an IrO_x/TaON photoanode and CdS/$CuInS_2$ photocathode was attempted. Fig. 4 shows the time dependence of NADH production with the photoelectrochemical cell consisting of an IrO_x/TaON photoanode and CdS/$CuInS_2$ photocathode.

Photocurrent density decreased from −0.19 to −0.15 mA cm^{-2} during the first 2 min of irradiation and then remained almost constant for 120 min, as shown in the inset of Fig. 4. As shown in Fig. S3,† using the system including a combination of CdS/$CuInS_2$ photocathode and IrO_x/TaON photoanode in the presence of $[Cp^*Rh(bpy)(H_2O)]^{2+}$, a current of approximately −0.15 mA cm^{-2} was predicted to be observed without any external bias, consistent with the experimentally observed current value shown in Fig. 4. The amount of NADH produced linearly increased with irradiation time when using this system. The yield of NADH from NAD^+ was estimated to be 8% at 120 min of irradiation. Here, the irradiation intensity from the light source onto the electrode surface was *ca.* 680 mW cm^{-2} (Fig. S4†). The light energy conversion efficiency for NADH production after 120 min of irradiation was estimated to be *ca.* 0.013%. Thus, NADH regeneration using a photoelectrochemical cell consisting of IrO_x/TaON photoanode and CdS/$CuInS_2$ photocathode was accomplished.

Finally, photoelectrochemical production of L-lactate *via in situ* NADH regeneration was performed by deploying a combination of a cocatalyst-loaded TaON photoanode and a CdS/$CuInS_2$ photocathode without an external bias. The photocurrent over this combination was found to depend on the onset potential of photocurrent over the TaON photoanode. As shown in Fig. S5,† all combinations showed relatively stable photocurrents without an external bias for 2 h of irradiation, while the photocurrent was quite low in the case of the CoO_x/TaON photoanode, which showed the most positive onset potential. The IrO_x/TaON photoanode, which showed the most negative onset potential, exhibited the highest photocurrent. Fig. 5 shows the time courses of the amounts of products over the system including a combination of the IrO_x/TaON photoanode and CdS/$CuInS_2$ photocathode under visible-light irradiation without an external bias. L-Lactate and O_2 were produced simultaneously during the 2 h of irradiation. The induction period observed for the O_2 evolution was mainly due to a time lag caused by the analysis method used. The amount of evolved H_2 was negligibly low (0.2 μmol for 2 h irradiation). Neither production of L-lactate nor of O_2 was observed under dark conditions, and when only the IrO_x/TaON photoanode was irradiated. Faradaic efficiencies for L-lactate and O_2 productions were estimated to be 92% and 93%, respectively, indicating that most of the photogenerated holes in TaON were consumed for water oxidation and most of the photoexcited electrons in CdS/$CuInS_2$ were consumed for L-lactate production through a pathway involving $[Cp^*Rh(bpy)(H_2O)]^{2+}$, the NAD^+/NADH redox couple and LDH. The results of the experiments using,

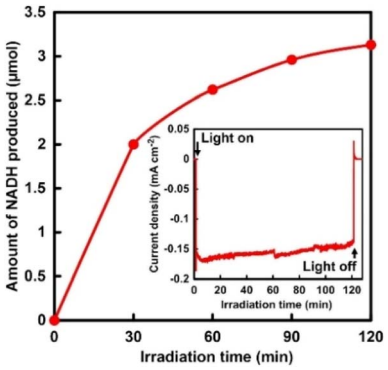

Fig. 4 Time dependence of NADH production using a system including a combination of a CdS/$CuInS_2$ photocathode, IrO_x/TaON photoanode and $[Cp^*Rh(bpy)(H_2O)]^{2+}$ under visible-light irradiation without an external bias. Inset: time dependence of photocurrent density.

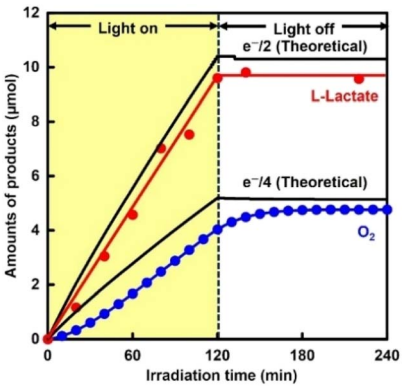

Fig. 5 Time dependence of amounts of L-lactate and O_2 produced over a system including a combination of a CdS/$CuInS_2$ photocathode, IrO_x/TaON photoanode and $[Cp^*Rh(bpy)(H_2O)]^{2+}$ under visible-light irradiation without an external bias.

respectively, the CoO_x/TaON and RhO_x/TaON photoanodes are shown in Fig. S6.† The photocurrent values obtained were consistent with those predicted from the current–potential curve for the respective photoanode and cathode. The case of the RhO_x/TaON or CoO_x/TaON photoanode showed simultaneous production of L-lactate and O_2, although the production rate using the RhO_x/TaON photoanode was lower than that when using IrO_x/TaON. From these results, visible-light–driven electrochemical production of L-lactate *via* NADH regenerated *in situ* and using water as an electron source was accomplished by deploying a combination of the IrO_x/TaON (or RhO_x/TaON) photoanode and CdS/$CuInS_2$ photocathode without an external bias. Using the combination of the IrO_x/TaON photoanode and CdS/$CuInS_2$ photocathode, NADH regeneration was achieved without the need for a sacrificial reductant under conditions without external bias, but a gradual decrease in photocurrent was observed with irradiation for a long period of time. It has been reported that a stable photocurrent can be obtained in a reduction system using methyl viologen as an electron mediator and a CdS/$CuInS_2$ photocathode.[26] In contrast, TaON-based photoanodes have been reported to become gradually deactivated due to factors such as changes in the pH of the solution.[29] It is expected that a future development of a TaON-based photoanode that is durable against light irradiation will lead to the construction of a stable and sustainable NADH regeneration system.

In summary, visible-light–driven electrochemical NADH regeneration using water as an electron source, enabled by a combination of an IrO_x/TaON (or RhO_x/TaON) photoanode and CdS/$CuInS_2$ photocathode without an external bias was demonstrated for the first time to the best of our knowledge. The CdS/$CuInS_2$ photocathode exhibited a cathodic photocurrent derived from reduction of $[Cp^*Rh(bpy)(H_2O)]^{2+}$ at a potential more negative than 0.03 V *vs.* Ag/AgCl. Reduction of NAD^+ to NADH proceeded *via* reduction of $[Cp^*Rh(bpy)(H_2O)]^{2+}$ over the CdS/$CuInS_2$ photocathode at a potential of −0.2 V *vs.* Ag/AgCl under visible-light irradiation. This NADH regeneration system can be applied to production of L-lactate from pyruvate using LDH. L-Lactate was stably produced over an extended period (30 h), reaching a total amount of 78 μmol, which exceeded the amounts of $[Cp^*Rh(bpy)(H_2O)]^{2+}$, NAD^+ and LDH that were used in the system. The introduction of the IrO_x/TaON (or RhO_x/TaON) photoanode enabled the visible-light–driven electrochemical production of L-lactate *via* NADH regenerated *in situ* using water as an electron source without an external bias.

Most photoelectrochemical NADH generation systems consist of a photocathode and a counter electrode such as platinum, and require an external bias[32,33] or a sacrificial reagent such as TEOA[34,35] to produce NADH. The system including the combination of the IrO_x/TaON photoanode and CdS/$CuInS_2$ photocathode in this study is a Z-scheme process similar to oxygenic natural photosynthesis using photosystems I and II, and has an advantage over other systems in that it uses water as an electron donor and can regenerate NADH without requiring an external bias. Thus, this study has made available a system including a combination of photoanode and photocathode for sustainable NADH regeneration and subsequent biocatalytic reactions.

Data availability

The authors confirm that the data supporting the findings of this manuscript are available within the article and its ESI.†

Conflicts of interest

There are no conflicts to declare.

Acknowledgements

This work was partially supported by the Japan Association for Chemical Innovation (JACI), Institute for Fermentation, Osaka (IFO) (G-2023-3-050), a Grant-in-Aid for Specially Promoted Research (23H05404), Scientific Research (B) (22H01872), (22H01871), Scientific Research (c) (21K05245), and the Fund for the Promotion of Joint International Research (Fostering Joint International Research (B)) (19KK0144, 20KK0116).

Notes and references

1 K. E. Taylor and J. B. Jones, *J. Am. Chem. Soc.*, 1976, **98**, 5689.
2 J. B. Jones, D. W. Sneddon, W. Higgins and A. J. Lewis, *J. Chem. Soc. Chem. Commun.*, 1972, 856.
3 A. Dibenedetto, P. Stufano, W. Macyk, T. Baran, C. Fragale, M. Costa and M. Aresta, *ChemSusChem*, 2012, **5**, 373.
4 F. Hollmann, I. W. C. E. Arends and K. Buehler, *ChemCatChem*, 2010, **2**, 762.
5 S. Immanuel, R. Sivasubramanian, R. Gul and M. A. Dar, *Chem.–Asian J.*, 2020, **15**, 4256.
6 E. Siu, K. Won and C. B. Park, *Biotechnol. Prog.*, 2007, **23**, 293.
7 I. Ali, T. Khan and S. Omanovic, *J. Mol. Catal. A:Chem.*, 2014, **387**, 86.
8 J. Kiwi, *J. Photochem.*, 1981, **16**, 193.
9 H. Y. Lee, J. Ryu, J. H. Kim, S. H. Lee and C. B. Park, *ChemSusChem*, 2012, **5**, 2129.
10 J. Liu and M. Antonietti, *Energy Environ. Sci.*, 2013, **6**, 1486.
11 K. T. Oppelt, E. Wöß, M. Stiftinger, W. Schöfberger, W. Buchberger and G. Knör, *Inorg. Chem.*, 2013, **52**, 11910.
12 D. Yadav, R. K. Yadav, A. Kumar, N. J. Park and J. O. Baeg, *ChemCatChem*, 2016, **8**, 3389.
13 R. K. Yadav, J. O. Baeg, G. H. Oh, N. J. Park, J. J. Kong, J. Kim, D. W. Hwang and S. K. Biswas, *J. Am. Chem. Soc.*, 2012, **134**, 11455.
14 R. K. Yadav, G. H. Oh, N. J. Park, A. Kumar, K. J. Kong and J. O. Baeg, *J. Am. Chem. Soc.*, 2014, **136**, 16728.
15 Y. Zhang, Y. Zhao, R. Li and J. Liu, *Sol. RRL*, 2021, **5**, 2000339.
16 J. Huang, M. Antonietti and J. Liu, *J. Mater. Chem. A*, 2014, **2**, 7686.
17 S. Fukuzumi, Y. M. Lee and W. Nam, *J. Inorg. Biochem.*, 2019, **199**, 110777.
18 X. Wang and H. H. P. Yiu, *ACS Catal.*, 2016, **6**, 1880.
19 H. C. Lo, O. Buriez, J. B. Kerr and R. H. Fish, *Angew. Chem., Int. Ed.*, 1999, **38**, 1429.

20 C. L. Pitman, O. N. L. Finster and A. J. M. Miller, *Chem. Commun.*, 2016, **52**, 9105.
21 R. Ruppert, S. Herrmann and E. Steckhan, *J. Chem. Soc. Chem. Commun.*, 1988, 1150.
22 E. Steckhan, S. Herrmann, R. Ruppert, J. Thömmes and C. Wandrey, *Angew. Chem., Int. Ed.*, 1990, **29**, 388.
23 A. Aljabour, D. H. Apaydin, H. Coskun, F. Ozel, M. Ersoz, P. Stadler, N. S. Sariciftci and M. Kus, *ACS Appl. Mater. Interfaces*, 2016, **8**, 31695.
24 S. Ikeda, T. Nakamura, S. M. Lee, T. Yagi, T. Harada, T. Minegishi and M. Matsumura, *ChemSusChem*, 2011, **4**, 262.
25 I. Tsuji, H. Kato and A. Kudo, *Chem. Mater.*, 2006, **18**, 1969.
26 T. Toyodome, Y. Amao and M. Higashi, *New J. Chem.*, 2021, **45**, 14803.
27 R. Abe, M. Higashi and K. Domen, *J. Am. Chem. Soc.*, 2010, **132**, 11828.
28 M. Higashi, K. Domen and R. Abe, *J. Am. Chem. Soc.*, 2012, **134**, 6968.
29 M. Higashi, Y. Kato, Y. Iwase, O. Tomita and R. Abe, *J. Photochem. Photobiol., A*, 2021, **419**, 113463.
30 S. M. Lee, S. Ikeda, T. Yagi, T. Harada, A. Ennaoui and M. Matsumura, *Phys. Chem. Chem. Phys.*, 2011, **13**, 6662.
31 H. Kumagai, T. Minegishi, Y. Moriya, J. Kubota and K. Domen, *J. Phys. Chem. C*, 2014, **118**, 16386.
32 N. Li, J. You, L. Huang, H. Zhang, X. Wang, L. He, C. Gong, S. Lin and B. Zhang, *Green Chem.*, 2023, **25**, 5247.
33 W. S. Choi, S. H. Lee, J. W. Ko and C. B. Park, *ChemSusChem*, 2016, **9**, 1559.
34 J. H. Kim, M. Lee, J. S. Lee and C. B. Park, *Angew. Chem., Int. Ed.*, 2012, **51**, 517.
35 E. J. Son, Y. W. Lee, J. W. Ko and C. B. Park, *ACS Sustainable Chem. Eng.*, 2019, **7**, 2545.